Synthesis and Properties of Homogeneously Dispersed Polyamide 6/MWNTs Nanocomposites via Simultaneous *In Situ* Anionic Ring-Opening Polymerization and Compatibilization

Dongguang Yan,[1,2] Guisheng Yang[1,3]

[1]*CAS Key Laboratory of Engineering Plastics, Joint Laboratory of Polymer Science and Materials, Institute of Chemistry, The Chinese Academy of Sciences, Beijing 100190, People's Republic of China*
[2]*Graduate School of the Chinese Academy of Sciences, Beijing 100039, People's Republic of China*
[3]*Shanghai Genius Advanced Materials Co., Ltd, Shanghai 201109, People's Republic of China*

Received 19 May 2008; accepted 24 November 2008
DOI 10.1002/app.29783
Published online 11 March 2009 in Wiley InterScience (www.interscience.wiley.com).

ABSTRACT: Toluene 2, 4-diisocyanate (TDI) functionalized multiwalled carbon nanotubes (MWNTs-NCO) were used to prepare monomer casting polyamide 6 (MCPA6)/MWNTs nanocomposites via *in situ* anionic ring-opening polymerization (AROP). Isocyanate groups of MWNTs-NCO could serve as AROP activators of ε-caprolactam (CL) in the *in situ* polymerization. Fourier transform infrared (FTIR) showed that a graft copolymer of PA6 and MWNTs was formed in the *in situ* polymerization. MWNTs-PA6 covalent bonds of the graft copolymer constituted a strong type of interfacial interaction in the nanocomposites and increased the compatibility of MWNTs and MCPA6 matrix. The nanocomposites were characterized for the morphology, mechanical, crystallization, and thermal properties through field emission transmission electron microscopy (FETEM), tensile testing, differential scanning calorimeter (DSC), and thermogravimetric analysis (TGA). FETEM analysis showed that MWNTs were homogeneously dispersed in MCPA6 matrix. The initial tensile strengths and tensile modulus of the nanocomposite with 1.5 wt % loading of MWNTs were enhanced by about 16 and 13%, respectively, compared with the corresponding values for neat MCPA6. DSC analysis indicated that the crystallization temperature of the nanocomposites was increased by 8°C by adding 1.5 wt % MWNTs compared with pure MCPA6. Besides, it was found that the thermal stability of MCPA6 was improved by the addition of the MWNTs. J Appl Polym Sci 112: 3620–3626, 2009

Key words: carbon nanotubes; polyamides; nanocomposites; *in situ* polymerization; *in situ* compatibilization

INTRODUCTION

Carbon nanotubes (CNTs) were discovered in 1991 and could be classified into two types: singlewalled carbon nanotubes (SWNTs) and multiwalled carbon nanotubes (MWNTs).[1] Because of their nanometer size, high aspect ratios, and more importantly, their extraordinary mechanical strength, and high electrical and thermal conductivity, polymer nanocomposites based on CNTs have attracted much academic and industrial interest as researchers strive to enhance the polymeric material properties via nanoscale reinforcement.[2–8]

There are three main approaches to prepare polymer/CNTs nanocomposites: (a) melt extrusion,[2,3] (b) *in situ* polymerization,[5–8] and (c) solution mixing.[9–13] However, the development of such nanocomposites has been impeded by the dispersion of CNTs in polymers matrix because of the strong intramolecular forces that exist between CNTs. The extended π-electron system of CNTs is highly polarizable, which results in significant attraction between nanotubes via Van der Waal forces. These Van der Waal forces are responsible for the formation of nanotube bundles, which are difficult to exfoliate because the nanotubes may be hundreds to thousands of nanometers long, impeding the uniform dispersion of the nanotubes in polymers matrix. Recently, to improve the chemical compatibility between polymers and CNTs, a number of research groups have focused on the functionalization of CNTs through both covalent and noncovalent approaches. Noncovalent functionalization includes surfactant modification,[14] polymer wrapping.[15–17] Covalent functionalization may roughly be divided into two categories: a direct attachment of functional groups to the graphitic surface[18–21] and the esterification or amination of the nanotube-bound carboxylic acids that come from intrinsic or induced defects by acid oxidation.[22] Polyamide 6 (PA6) is an important thermoplastic with a wide range of engineering applications. Acid-

Correspondence to: G. S. Yang (ygs@geniuscn.com).

and amine-functionalized CNTs have been successfully used to prepare PA6/CNTs nanocomposites via melt extrusion or *in situ* hydrolytic polymerization.[2,3,5,13,17,23–27] Because of super high molecular weight and high degree of crystallization, monomer casting polyamide 6 (MCPA6) has more advantages over normal polycondensation PA6.[11] However, very few reports were concerned about preparation of monomer casting polyamide 6 (MCPA6)/MWNTs nanocomposites via *in situ* AROP of ε-caprolactam.

In this study, we demonstrate a novel route to prepare MCPA6/MWNTs nanocomposites. First, commercial hydroxyl functionalized multiwalled carbon nanotubes (MWNTs-OH) were functionalized by toluene 2, 4-diisocyanate (TDI) through esterification. Second, TDI functionalized MWNTs (MWNTs-NCO) were used as *in situ* activators for anionic ring-opening polymerization (AROP) of ε-caprolactam (CL) to prepare MCPA6/MWNTs nanocomposites. It is expected that PA6 chains can grow from the sidewalls of the MWNTs, and the grafted PA6 can act as *in situ* compatibilizers, which results in homogeneous dispersion of MWNTs in the MCPA6 matrix. The chemical structure of MWNTs-NCO and PA6 grafted MWNTs (MWNTs-PA6) was confirmed by Fourier transform infrared (FTIR). Dispersion state of MWNTs in MCPA6 was characterized by field emission transmission electron microscope (FETEM). The effect of MWNTs on the tensile, crystallization, and thermal stability of MCPA6 was investigated.

EXPERIMENTAL

Materials

Commercial grade CL was obtained from Nanjing Oriental Chemical Company and dried in vacuum at 140°C for 20 min to remove trace water before use. MWNTs-OH (3.06 wt % OH) were purchased from Chengdu Organic Chemistry Co., purity > 95 wt %, diameter 10–20 nm, length ~ 30 μm. ε-Caprolactam sodium salt (CLNa) (Bruggolen® C10, Brüggemann Chemical) acted as catalyst for AROP. TDI, toluene, and *N*,*N*-dimethylformamide (DMF) were received from Sinopharm Chemical Reagent Co. Toluene and DMF were both dried over $CaSO_4$ and redistilled before use.

Preparation of MWNTs-NCO

MWNTs-NCO were obtained by attaching TDI to MWNTs-OH via chemical methods, and the detailed procedures followed a previous route.[28] About 100 mg of MWNTs-OH was dispersed in 50 mL of TDI under stirring, and the functionalization was undertaken in a dry nitrogen atmosphere at 80°C for 72 h. The obtained MWNTs-NCO were filtrated and washed three times with toluene, and then subjected to a 48 h Soxhlet extraction with DMF to completely remove the unreacted TDI. After being dried in vacuum at 40°C for 24 h, MWNTs-NCO were obtained.

In situ preparation of MCPA6/MWNTs nanocomposites

Desired amount of MWNTs-NCO was added to a solution of 80 g CL and 20 g DMF, and a stable liquid mixture was obtained with the aid of ultrasonic for 1 h at room temperature. Afterward, most of the DMF was removed via vacuum distillation at 60°C, and then, the mixture was heated at 170°C under vacuum for another 20 min to remove trace amount of DMF. Finally, appropriate amount of TDI was added to assure that the content of the isocyanate groups in all preparation was identical. After adding 4 wt % CLNa, the final mixture was immediately poured into a preheated mold in an air-circulating oven at 160°C and polymerized for 10 min. Then, the products were cooled in an oven at 40°C, and MCPA6/MWNTs nanocomposites with various contents of MWNTs-NCO (0.5, 1.0, and 1.5 wt %) were obtained. MCPA6/raw MWNTs-OH nanocomposites were also prepared following the above procedure.

Characterization

Fourier transform infrared

To characterize the chemical structure of MWNTs in the MCPA6/MWNTs nanocomposites, the MWNTs, which were named MWNTs-PA6, were extracted from the nanocomposites. The extraction procedure was as follows. The nanocomposites were dissolved in formic acid and carefully washed by formic acid several times to remove physically absorbed MCPA6 on the surface of MWNTs. After being dried in vacuum at 80°C for 24 h, the MWNTs-PA6 were obtained. FTIR spectra of MWNTs-OH, MWNTs-NCO, and MWNTs-PA6 was recorded using KBr tablets on a Nicolet Avater-360 FTIR spectrometer in the range 4000 to 500 cm^{-1}, with a resolution of 4 cm^{-1} at room temperature.

Field emission transmission electron microscope

The surface morphology of MWNTs-OH and MWNTs-PA6 was measured by a FETEM (JEM-2100F, JEOL).[12] MWNTs-OH and MWNTs-PA6 were firstly dispersed in formic acid by the aid of ultrasonic for 10 min. Then, a droplet of formic acid solution was dripped onto a holey carbon-coated copper grid, followed by solvent evaporation. The morphology of the nanocomposites was also measured by FETEM. The samples were ultramicrotomed with a diamond knife on a Leica Ultracut UCT microtomed at −20°C to give

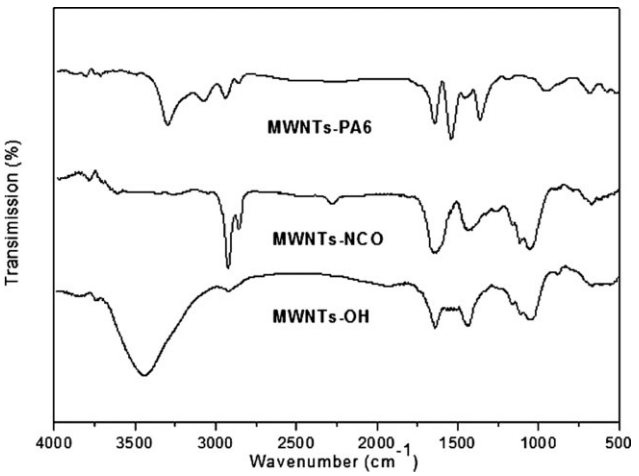

Figure 1 FTIR spectra of MWNTs-OH, MWNTs-NCO, and MWNTs-PA6.

70-nm thick sections. The sections were transferred to carbon-coated Cu grids of 200 meshes.

Tensile properties measurement

The MCPA6/MWNTs nanocomposites were directly carved into standard testing specimens of length 75 mm, parallel length 25 mm, gauge width 4 mm, and thickness 2 mm. Tensile tests were performed on an Instron machine series 1122 according to the DIN 53504 with a crosshead speed of 50 mm/min. Test results reported were the average values of at least five.

Differential scanning calorimeter

Differential scanning calorimeter (DSC) measurements were carried out on a NETZSCH DSC 200 PC calibrated in standards. All the measurements were performed from room temperature to 280°C at a heating rate of 10°C/min under nitrogen atmosphere. Samples were held at 280°C for 5 min to erase any previous thermal history, and then underwent subsequent cooling and heating cycles at a rate of 10°C/min.

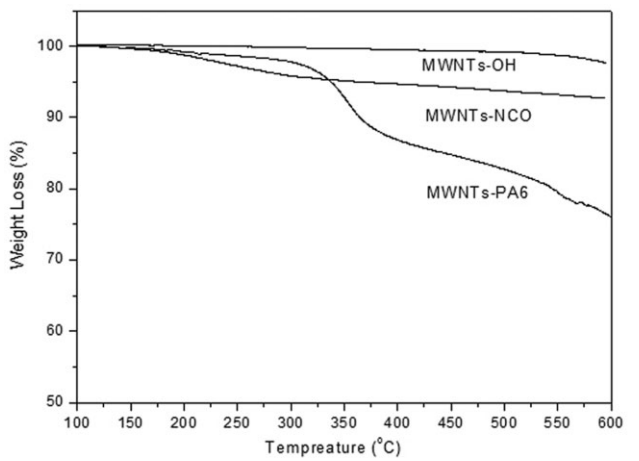

Figure 2 TGA curves of MWNT-OH, MWNT-NCO, and MWNTs-PA6.

Thermogravimetric analysis

Weight loss of MWNTs-OH, MWNTs-NCO, and MWNTs-PA6 was measured by SDTQ600 (USA TA Instrument Corp.) using platinum pans to determine the grafting amount of TDI and PA6, respectively, on MWNTs. The samples were heated from 50 to 600°C at a rate of 20°C/min under nitrogen flow of 20 mL/min.

The thermal decomposition studies of pure MCPA6 and nanocomposites were performed over a temperature range of 50 to 600°C using a TA instrument SDT Q600 under nitrogen environments.

RESULTS AND DISCUSSION

Grafting TDI and growing PA6 chains onto the surface of MWNTs

Infrared spectroscopy is an important means for confirming the chemical grafting to the surfaces of

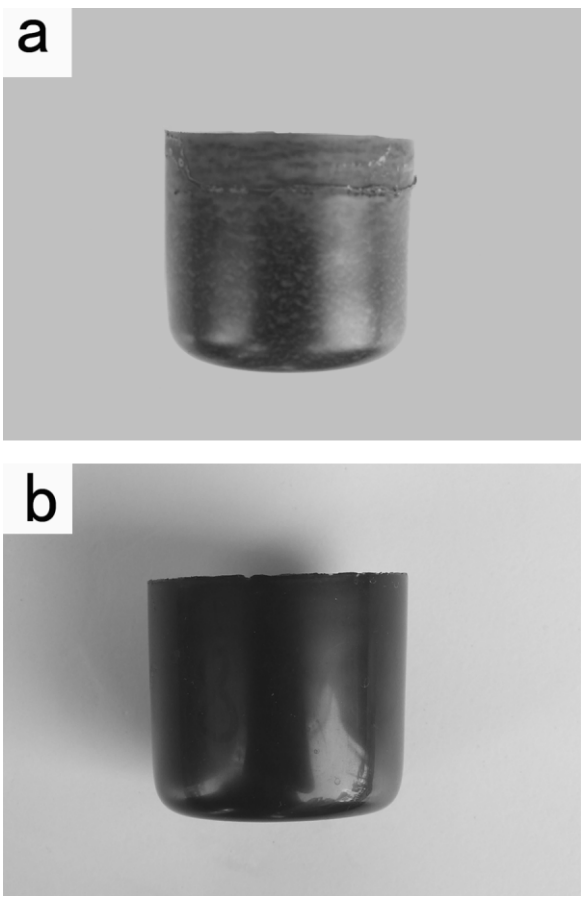

Figure 3 Digital photographs of MCPA6/raw MWNTs-OH nanocomposites (a) and MCPA6/MWNTs nanocomposites.

CNTs. Figure 1 showed FTIR spectra of MWNTs-OH, MWNTs-NCO, and MWNTs-PA6. For MWNTs-OH, the peak appearing around 3400 cm^{-1} was attributed to the O—H stretching of the hydroxyl groups of MWNTs-OH. However, for MWNTs-NCO, the characteristic peak of hydroxyl groups disappeared. A new peak at 2283 cm^{-1} was found, which corresponded to the asymmetric stretching of isocyanate groups. The peaks at 2900 and 2825 cm^{-1} were due to the C—H stretching of methyl groups of TDI. The peak 1245 cm^{-1} was ascribed to C—N stretching of carbamate groups resulting from the esterification of hydroxyl and isocyanate groups.[28] Thus, the FTIR spectra results suggested that TDI had been successfully grafted onto MWNTs to form MWNTs-NCO. In the FTIR spectra of MWNTs-PA6, compared with MWNTs-NCO, the disappearance of the peak at 2283 cm^{-1} indicated that isocyanate groups had been consumed during the *in situ* anionic ring-opening polymerization. Furthermore, the characteristic absorption bands for PA6 were all observed, for example, the absorption peaks at 3297 (NH stretching), 3060, 1637 (amide I band), and 1540 cm^{-1} (amide II band). The FTIR results verify that the PA6 chains are covalently attached to MWNTs due to the activation of isocyanate groups for AROP of ε-caprolactam.

To gain quantitative information of the extent of MWNTs functionalization, thermogravimetric analysis (TGA) under nitrogen environment was performed on the MWNTs, MWNTs-NCO and MWNTs-PA6 as depicted in Figure 2. MWNTs did not exhibit large weight loss until 550°C. Comparatively, for MWNTs-NCO and MWNTs-PA6, major decomposition took place at a temperature that ranged from 200 to 500°C corresponding to the surface grown TDI and PA6.[28,29] If the mass loss of the MWNT-OH at 550°C is used as the reference, the

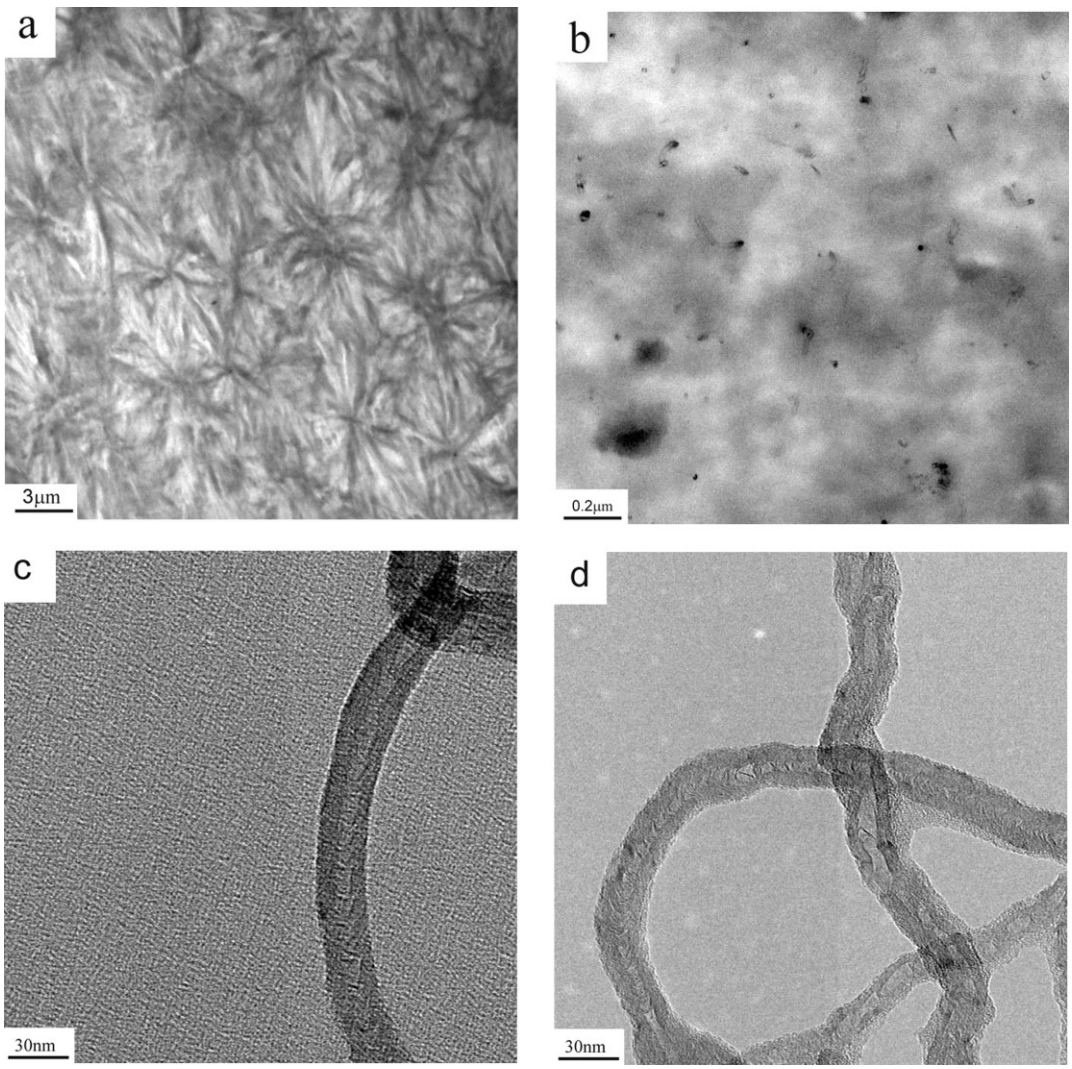

Figure 4 FETEM images of MCPA6/MWNTs nanocomposites (a, b), raw MWNTs-OH, (c) and MWNTs-PA6 (d).

TABLE I
Tensile Properties of MCPA6 and MCPA6/MWNTs Nanocomposites

MWNTs content (wt %)	Tensile strength (MPa)	Tensile modulus (MPa)	Elongation at break (%)
0	58.7 ± 0.5	815 ± 50	125 ± 6
0.5	60.1 ± 0.4	834 ± 30	106 ± 3
1.0	66.5 ± 0.6	962 ± 70	99 ± 5
1.5	68.0 ± 0.5	923 ± 50	91 ± 2

amount of TDI and PA6 covalently attached to MWNTs determined by TGA is about 8.0 and 21.5 wt %, respectively, as shown in Figure 2.

Morphology of MCPA6/MWNTs nanocomposites

The digital pictures of MCPA6/raw MWNTs-OH and MCPA6/MWNTs nanocomposites are shown in Figure 3. MCPA6/raw MWNTs-OH nanocomposites were macroscopically heterogeneous from Figure 3(a). The aggregates of raw MWNTs-OH could be seen with naked eyes. However, it can be seen that MCPA6/MWNTs nanocomposites were macroscopically homogenous from Figure 3(b).

FETEM images of MCPA6/MWNTs nanocomposites were shown in Figure 4(a,b). Radial textures with black spots at their centers were homogeneously dispersed in the MCPA6 matrix, as shown in Figure 4(a). These radial textures were attributed to the spherulitic morphology of MCPA6 crystals, which had been confirmed by us.[29] Figure 4(b) showed that the black spots were well dispersed MWNTs. These results indicate that the dispersion of MWNTs in MCPA6 matrix is homogeneous.

Figure 4(c,d) showed the surface nanostructures of raw MWNTs-OH and MWNTs-PA6. Figure 4(c) revealed that the surface of the raw MWNTs-OH was relatively smooth and clean. However, the surface of MWNTs-PA6 was obviously different [Fig. 4(d)] from the raw one, because it was coarse and coated by a layer of polymer. The fact that this layer cannot be washed away by formic acid was because of the grafting copolymerization of PA6 onto the MWNTs. The isocyanate groups on the MWNTs-NCO could react with the amide groups of ε-caprolactam to form acyl caprolactam, which would activate the AROP of CL.[28] PA6 chains would grow from the surface of MWNTs, and grafting copolymers of MWNTs and PA6 were formed in the *in situ* polymerization. The grafted PA6 chains would penetrate and bridge the connection of the MWNTs to the MCPA6 matrix, thereby increasing the compatibility and propelling the original MWNTs to be exfoliated into individual tubes in the *in situ* polymerized MCPA6 matrix. The dispersibility of MWNTs in MCPA6 matrix was remarkably improved when compared with raw MWNTs-OH, as shown in Figure 3.

Tensile properties

The tensile properties of MCPA6 and MCPA6/MWNTs nanocomposites are given in Table I. It could be seen that addition of MWNTs significantly improved the tensile properties of MCPA6 matrix. Table I showed that the tensile strength and modulus were increased from 58.7 (MCPA6) to 68.0 MPa (MCPA6/MWNTs nanocomposites) and from 815 (MCPA6) to 923 MPa (MCPA6/MWNTs nanocomposites), respectively, by the incorporation of 1.5 wt % MWNTs into MCPA6 matrix. However, elongation at the break decreased gradually when the amount of MWNTs increased in the nanocomposites. The enhancement of the tensile strength and modulus of the MCPA6/MWNTs nanocomposites could be attributed to the reinforcement effect of MWNTs with a high aspect ratio and their uniform

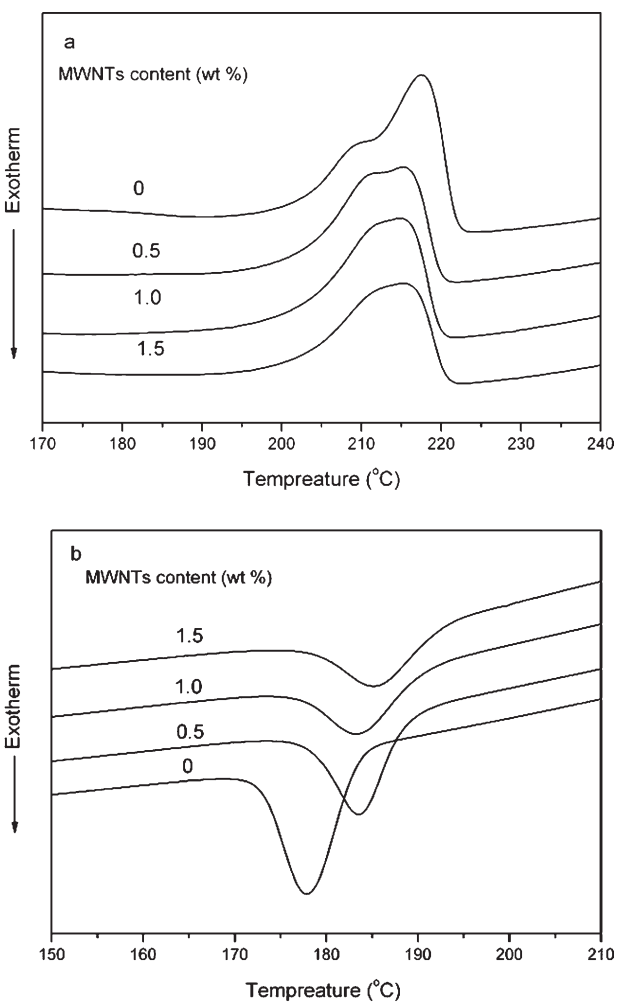

Figure 5 Thermograms of pure MCPA6 and nanocomposites with various amounts of MWNTs. (a) the second heating; (b) cooling.

TABLE II
Characteristic Values of Crystallization and Melting Behavior of MCPA6 and Nanocomposites with Various Amounts of MWNTs

	Heating (2nd)			Cooling		
MWNTs content (wt %)	Onset (°C)	T_m (°C)	ΔT_m (°C)	ΔH_c (J·g^{-1})	$T_{c,m}$ (°C)	ΔT_d (°C)
0	207	217	14	45.5	178.5	38.5
0.5	209	215	10	43.7	182.3	32.7
1.0	209	215	10	42.9	185.3	29.7
1.5	209	215	10	40.5	186.5	28.5

dispersion in MCPA6 matrix. The elongation at break (about 91%) slightly decreased, indicating that the composite became somewhat brittle compared with neat MCPA6 (which breaks at above 125% of elongation).

Crystallization behavior of MCPA6/MWNTs nanocomposites

DSC analysis was performed on pure MCPA6 and nanocomposites with MWNTs contents of 0.5, 1.0, and 1.5 wt %, respectively. The results of DSC heating and cooling scans were shown in Figure 5 and Table II. The melting onset temperature and melting peak width (ΔT_m) are related to the least stability and distribution of crystallites, respectively. An increase of the melting onset temperature and a decrease of ΔT_m were found in the nanocomposites with respect to that of pure MCPA6. The values of melting onset temperature for all nanocomposites (209°C) were 2°C higher than that of pure MCPA6 (207°C). The values of ΔT_m for the nanocomposites were 4°C lower than that of pure MCPA6. These results indicated that the crystallites in the nanocomposites were more perfect, and the size distribution of the crystallites in the nanocomposites was more homogeneous than that in pure MCPA6.

The crystallization peak temperature (T_c) represents the temperature at the maximum crystallization rate. Also, these temperatures for the nanocomposites were higher by 4 to 8°C than that of pure MCPA6 (185°C). The crystallization peak width (ΔT_c) and the heat of crystallization (ΔH_c) are related to the overall crystallization rate and the degree of crystallization, respectively. The ΔT_c for the nanocomposites were narrower by 4 to 10°C than that of pure MCPA6 (38.5°C). These results implied that the crystallization of MCPA6 could be accelerated by the incorporation of MWNTs, which could be explained by the heterogeneous nucleation effect of the MWNTs. However, the ΔH_c was decreased slightly with the increasing MWNTs content, which meant that the degree of crystallization of the nanocomposites was a little lower than that of pure MCPA6. The probable reason may be that the covalent links between MWNTs and PA6 increased the steric hindrance and prevented the PA6 molecular chain from arranging in order.

Thermal stability

The thermal gravimetric analysis (TGA) weight loss and derivative thermograms (DTG) for MCPA6 and MCPA6/MWNTs nanocomposites under nitrogen environment were presented in Figure 6. The decomposition process of both pure MCPA6 and

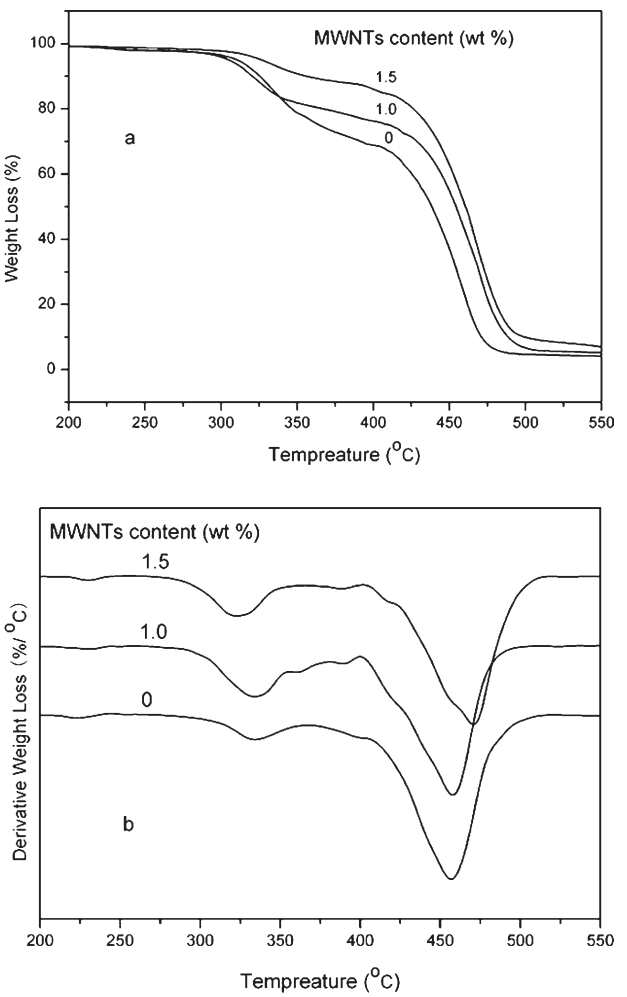

Figure 6 TGA (a) and DTG (b) curves of pure MCPA6 and nanocomposites with various amounts of MWNTs under nitrogen environment.

nanocomposites can be divided into two stages (Fig. 6), which was similar with the results in our previous work.[30] The first peak probably attributed to the fact that a few remnants of CL monomer in the matrix induce the decomposition of MCPA6 at a lower temperature. The second stage corresponded to the thermal decomposition of MCPA6. The onset temperature and the temperatures at maximum mass loss rate for the second stage of the nanocomposites were both higher than those of the pure MCPA6, especially for the case of nanocomposites with 1.5 wt % MWNTs, which showed an improvement more than 10°C. As we all know, the MWNTs could effectively inhibit the thermal degradation of PA6 due to shielding effect.[31] In our cases, the excellent interface affinity between MWNTs and MCPA6 matrix could further facilitate this shielding effect and thus improve the thermal stability of the nanocomposites.

CONCLUSIONS

MWNTs-NCO were ideal nanofillers to prepare homogeneously dispersed MCPA6/MWNTs nanocomposites via the *in situ* AROP. PA6 molecular chains covalently attached to the sidewalls of MWNTs could act as *in situ* compatibilizers in the nanocomposites and enhance the dispersion of MWNTs. The uniformly dispersed MWNTs improved the tensile properties because of the reinforcement effect. Because of the heterogeneous nucleation effect of MWNTs, the crystallization capacity of MCPA6/MWNTs nanocomposites was improved remarkably. The MWNTs coated by PA6 had an excellent ability of inhibiting the thermal degradation of the nanocomposites, and thus improved the thermal stability of the nanocomposites under nitrogen.

References

1. Iijima, S. Nature 1991, 354, 56.
2. Liu, T. X.; Phang, I. Y.; Shen, L.; Chow, S. Y.; Zhang, W. Macromolecules 2004, 37, 7214.
3. Zhang, W. D.; Shen, L.; Phang, I. Y.; Liu, T. X. Macromolecules 2004, 37, 256.
4. Kalgaonkar, R. A.; Jog, J. P. Polym Int 2008, 57, 114.
5. Gao, C.; Jin, Y. Z.; Kong, H.; Whitby, R. L. D.; Acquah, S. F. A.; Chen, G. Y.; Qian, H. H.; Hartschuh, A.; Silva, S. R. P.; Henley, S.; Fearon, P.; Kroto, H. W.; Walton, D. R. M. J Phys Chem B 2005, 109, 1125.
6. Carlos, V. S.; Ana, L. M. H.; Frank, T. F.; Rodney, R.; Victor, M. C. Chem Mater 2003, 15, 4470.
7. Hu, N. T.; Zhou, H. W.; Dang, G. D.; Rao, X. H.; Chen, C. H.; Zhang, W. J. Polym Int 2007, 56, 655.
8. Lu, X. F.; Chao, D. M.; Zheng, J. N.; Chen, J. Y.; Zhang, W. J.; Wei, Y. Polym Int 2006, 55, 945.
9. Qu, L. W.; Veca, L. M.; Lin, Y.; Kitaygorodskiy, A.; Chen, B. L.; Sun, Y. P. Macromolecules 2005, 38, 10328.
10. Wu, H. L.; Wang, C. H.; Ma, C. C. M.; Chiu, Y. C. Compos Sci Technol 2007, 67, 1854.
11. Rusu, G.; Ueda, K.; Rusu, E.; Rusu, M. Polymer 2001, 42, 5669.
12. Zhao, B.; Hu, H.; Haddon, R. C. Adv Funct Mater 2004, 14, 71.
13. Krul, L. P.; Volozhyn, A. I.; Belov, D. A.; Poloiko, N. A.; Artushkevich, A. S. Biomol Eng 2007, 24, 93.
14. Jin, H. J.; Choi, H.; Yoon, S. H.; Myung, S. J.; Shim, S. E. Chem Mater 2005, 17, 4034.
15. Bose, S.; Bhattacharyya, A. R.; Kodgire, P. V.; Misra, A. Polymer 2007, 48, 356.
16. Einat, N. R.; Rina, S. C.; Céline, B.; Marc, F.; Zhang, D. S.; Szleifer, I.; Rachel, Y. R. Macromolecules 2007, 40, 3676.
17. Bhattacharyya, A. R.; Pötschke, P.; Häußler, L.; Fischer, D. Macromol Chem Phys 2005, 206, 2084.
18. Guo, G. Q.; Yang, D.; Wang, C. C.; Yang, S. Macromolecules 2006, 39, 9035.
19. Michelson, E. T.; Huffman, C. B.; Rinzler, A. G.; Smalley, R. E.; Hauge, R. H.; Margrave, J. L. Chem Phys Let 1998, 296, 188.
20. Michelson, E. T.; Chiang, I. W.; Zimmerman, J. L.; Boul, P. J.; Lozano, J.; Liu, J.; Smalley, R. E.; Hauge, R. H.; Margrave, J. L. J Phys Chem B 1999, 103, 4318.
21. Polona, U.; Jin, W. S.; Klara, H.; Ales, M.; Peter, P.; Dragan, D.; Mihailovic, L. S. F. Chem Mater 2003, 15, 4751.
22. Sun, Y. P.; Fu, K. F.; Lin, Y.; Huang, W. J Acc Chem Res 2002, 35, 1096.
23. Gao, J. B.; Itkis, M. E.; Yu, A. P.; Bekyarova, E.; Zhao, B.; Haddon, R. C. J Am Chem Soc 2005, 127, 3847.
24. Gao, B.; Zhao, B.; Itkis, M. E.; Bekyarova, E.; Hu, H.; Kranak, V. J Am Chem Soc 2006, 128, 7492.
25. Zhao, C. G.; Hua, G. J.; Justiceb, R. Polymer 2005, 46, 5125.
26. Sun, L.; Yang, J. T.; Lin, G. Y.; Zhong, M. Q. Mater Lett 2007, 61, 3963.
27. Li, J.; Fang, Z. P.; Tong, L. F.; Gu, A. J.; Liu, F. J Appl Polym Sci 2007, 106, 2898.
28. Yang, M.; Gao, Y.; Li, H.; Adronov, A. Carbon 2007, 45, 2327.
29. Yan D. G.; Xie T. X.; Yang G. S. J Appl Polym Sci 2009, 111, 1278.
30. Liu, A. D.; Xie, T. X.; Yang, G. S. Macromol Chem Phys 2006, 207, 701.
31. Saeed, K.; Park, S. Y. J Appl Polym Sci 2007, 106, 3729.